ELSEVIER

Journal of Power Sources 86 (2000) 274–282

JOURNAL OF POWER SOURCES

www.elsevier.com/locate/jpowsour

Use of stainless steel for cost competitive bipolar plates in the SPFC

Robert C. Makkus *, Arno H.H. Janssen, Frank A. de Bruijn, Ronald K.A.M. Mallant

Netherlands Energy Research Foundation, Department of Fuels, Conversion, and Environment, P.O. Box 1, 1755 ZG Petten, Netherlands

Accepted 26 October 1999

Abstract

Bipolar plate materials for the Solid Polymer Fuel Cell (SPFC), alternative to the presently used graphite, should fulfil the following requirements in order to be applicable: low-cost, easy to machine or to shape, lightweight and low volume, mechanically and sufficiently chemically stable, and having a low contact resistance. Stainless steel is a low-cost material that is easy to shape, and thin sheets can be used to yield low volume and weight. Several stainless steels have been tested for their applicability. The compaction pressure is of large influence on the contact resistance. Also, the pre-treatment of the surface is of influence; this is a permanent effect. Stainless steel constituents slowly dissolve into the Membrane Electrode Assembly (MEA). It has been found that the anode side stainless steel flow plate is the main source of contamination. Direct contact between the stainless steel and the membrane greatly enhances the contaminant level. Using an appropriate pre-treatment and a coating or gasket preventing direct contact between stainless steel and the membrane, one alloy was found to satisfy the requirements for use as a low cost material for the flow plate of an SPFC. © 2000 Elsevier Science S.A. All rights reserved.

Keywords: Solid Polymer Fuel Cell; Bipolar plate

1. Introduction

The Solid Polymer Fuel Cell (SPFC) or Polymer Electrolyte Membrane Fuel Cell (PEMFC) is a promising option as the power source for electrical vehicles. Furthermore, the use of SPFCs in micro-CHP systems is gaining more and more interest. Major drawbacks preventing large-scale introduction of SPFC-based systems for global transport applications are the high costs and the low power density of the fuel cell systems.

An important component contributing to the high cost and low power density is the bipolar plate in the fuel cell stack, which connects electrically the adjacent cells of the stack and which provides the gas supply to the cells. Presently, the most commonly used bipolar plate material is graphite. The advantages of graphite are its excellent resistance to corrosion, its low bulk resistivity, its low specific density, and its low electrical contact resistance with electrode backing materials. The disadvantages of graphite are its costs, the difficulty of machining it, and its brittleness. Due to the brittleness of graphite, the bipolar plates need to have a thickness in the order of several millimetres, which makes a fuel cell stack heavy and voluminous.

Alternative bipolar plate materials should fulfil the following requirements in order to be applicable: low-cost, easy to machine or to shape, lightweight and low volume, mechanically and sufficiently chemically stable, and having a low contact resistance. Several authors are presently investigating alternative materials for the bipolar plate: pure metals and stainless steels [1–6] either with or without a protective and conductive coating, and carbon composite materials [7–10]. Since 1994, ECN has been investigating the applicability of stainless steels for use as bipolar plate material [11].

Stainless steel is a low-cost material, it is easy to shape and sheets as thin as 0.2–1 mm can be used, thus yielding a low volume stack. The high material density is compensated by the possibility of using thin sheets. A major disadvantage can be its chemical instability in the fuel cell environment, especially when in direct contact with the acidic electrolytic membrane. Corrosion of the metal bipolar plate leads to a release of multivalent cations, which can both lead to an increase in membrane resistance [12] and to poisoning of the electrode catalysts. Direct contact between the stainless steel and the acidic membrane can, of course, be avoided by using a coating or a gasket at the edge of the cell.

* Corresponding author.

0378-7753/00/$ - see front matter © 2000 Elsevier Science S.A. All rights reserved.
PII: S0378-7753(99)00460-7

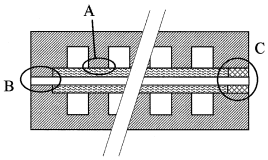

Fig. 1. Schematic of cell with areas of interest: (A) area with contact resistance between plate material and electrode; (B) area where direct contact between plate material and electrolyte occurs; (C) area where contact between plate and electrolyte is avoided by gasket or coating.

Another point of concern is the formation of passivating layers on the surface of stainless steels. Although protecting the bulk material against continuing corrosion, the result is an increased contact resistance between the bipolar plate and the electrode backing. This increase in contact resistance results in a power loss of the order of 2–5% per additional 25 $m\Omega\ cm^2$ compared to graphite.

The objective of this study is to identify stainless steels which have a sufficient chemical stability and a contact resistance no more than 25 $m\Omega\ cm^2$ higher than graphite. A special method has been developed to determine the contact resistance.

2. Experimental

The areas of interest when studying the suitability of bipolar plate materials for fuel cells are shown in Fig. 1.

The first aim of this study is to determine the suitability of stainless steels as bipolar plate material. For reasons of simplicity, the electrolyte membrane of the fuel cell can be used as a gasket per se, preventing the leakage of hydrogen and pressurised air to the surroundings. The consequence of this simple concept is, however, that there is a direct contact between the acidic membrane and the bipolar plate. Experiments have to determine whether this direct contact does lead to corrosion of the metal, and to detrimental effects on fuel cell performance. If this is the case, a gasket or coating can possibly prevent this local corrosion, the uncoated stainless steel only being exposed to the fuel cell electrode backing. In this fuel cell electrode backing/bipolar plate interface, the contact resistance is a matter of concern. A special technique has been developed for the constant monitoring of this contact resistance during the fuel cell operation.

2.1. Selection of candidate stainless steels and selection criteria

Candidate stainless steels have been selected on the basis of their commercial availability and elemental composition. The amount of chromium, nickel and molybdenum are known to have a marked influence on passivation and susceptibility to different types of corrosion. The stainless steels selected are listed in Table 1.

The criteria which a material has to meet in order to be selected as a bipolar plate candidate, are:

– low decay in current density: target value less than 10% in 5000 h;
– low total contact resistance: target value less than 50 $m\Omega\ cm^2$ after 5000 h;
– low release of contaminating cations: target value less than $8 \cdot 10^{-7}$ mol/cm^2 during 5000 h for a Nafion 117 membrane.

The amount of $8 \cdot 10^{-7}$ mol/cm^2 cations released corresponds to 5% exchange of electrolyte protons by metal ions in a Nafion 117 membrane.

2.2. Fuel cell experiments

Fuel cell experiments were performed under three different sets of conditions. The details are given in Table 2. For all experiments, Nafion 117 was used as the electrolytic membrane and Nafion impregnated E-tek Elat with a platinum loading of 0.35 mg cm^{-2} was used for both the anode and the cathode. Membrane Electrode Assemblies (MEAs), were prepared by hot-pressing the Nafion 117 and the Nafion impregnated E-tek electrodes together at a temperature of 130°C and a pressure of 35 bar(g) for 1.5 min.

In the stainless steel test samples, a single serpentine channel, 1 mm in depth and width, was machined. Following machining, the samples were cleaned and pickled.

Each test was duplicated. During the test, the current density and the voltage drop over the backing and the samples were continuously recorded. From this voltage drop the contact resistance between the electrode backing and the bipolar plate can be calculated.

All MEAs were post-test analysed for contaminants.

In all experiments, the materials were subjected to an alternating load, simulating the actual situation in an auto-

Table 1
Candidate stainless steels investigated and their elemental composition

Material UNS code	Fe (%)	C (%)	Cr (%)	Ni (%)	Mo (%)	N (%)	Mn (%)	Others (%)
1.4439	64	< 0.04	16–18	12–14	4–4.5	0.12–0.22	< 1.5	
1.4404 (316 L)	67	< 0.03	17–20	9–13	2–3	0.1–0.2	< 1.5	
1.4541	70	< 0.02	17–19	9–12			< 2	Ti < 0.8
1.4529	46	< 0.02	19–21	24–26	6–7	0.1–0.25	< 2	Cu: 0.5–1.5
1.3974	51	< 0.03	21–25	15–18	2.7–3.7	0.3–0.5	4.5–6.5	
Alloy A								
Alloy B								

Table 2
Conditions at the three different sets of fuel cell experiments

	High compaction pressure	Low compaction pressure	Long term stability tests
Compaction pressure (bar(g))	30	4	4
Cell geometry	Square, 7 cm^2	circular, 8 cm^2	circular, 8 cm^2
Flow pattern	Single serpentine, 1 mm wide/1mm deep	single serpentine, 1 mm wide/1mm deep	single serpentine, 1 mm wide/1mm deep
Bipolar plate/MEA interface	Direct contact BPP/membrane	only electrode backing in direct contact with BPP	only electrode backing in direct contact with BPP
Bipolar plate configuration	Anode and cathode plate stainless steel	anode and cathode plate stainless steel	only stainless steel at one fuel cell side, other side graphite
Cell temp. (°C)	80	80	65
Pressure (bar(a))	3	3	1.5
Dew point H_2 (°C)	90	80	65
Dew point air (°C)	85	80	65
Air stoichiometry	2.5	2	2
H_2 stoichiometry	2.5	1.5	1.5
Cell voltage (V)	0.5	0.5	0.5
Load/OCV time (min/min)	30/30	30/30	55/5

mobile. This subjects the stainless steel to a more severe condition, especially at the anode side, than when operated under constant load, as the change in anode potential changes the conditions from mild (under load) to severe (at OCV).

For the long term stability tests, the alternating load frequency was changed to 55 min at 0.5 V and 5 min at OCV, as during this study it became clear that the length of the OCV period influences the degradation of a cell.

In the first set of experiments, the stainless steel samples were positioned at both the anode and the cathode side of the MEA, and a high compaction pressure of 30 bar(g) was applied. The membrane provided the sealing, so the samples were in direct contact with the membrane. The materials were first tested in a square cell with an active area of 7 cm^2.

In the second series of experiments a smaller selection of stainless steels was tested in a different set-up. This set-up better represents the actual situation in a fuel cell stack: the hydrogen and air are humidified by passing over wet Nafion membranes, and the pressure used to seal the fuel cell components is restricted to 4 bar(g), as this more closely simulates the actual compaction pressure in the envisaged stack. Graphite and 1.4404 (316L) were tested under the same conditions and used as reference materials.

The test samples were used as an inlay in a gold-coated test fixture, i.e., only the active area consisted of the test material. No direct contact between the bipolar plate and the membrane occurred in these tests.

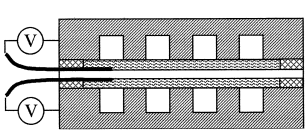

Fig. 2. Schematic of method for measuring the voltage drop over backing and contact with flow plate.

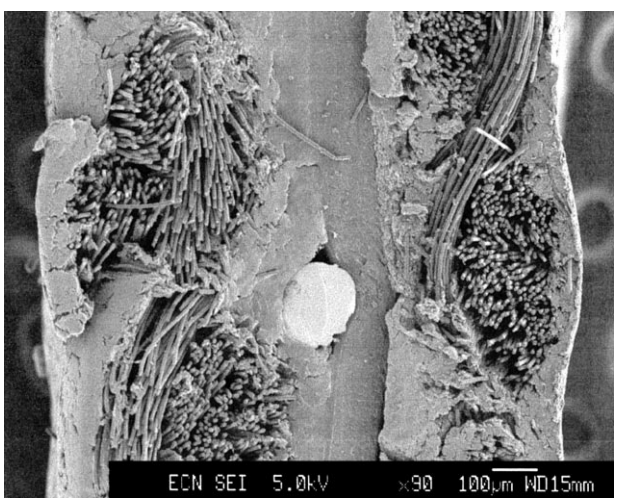

Fig. 3. Cross-section of a MEA including the gold wire. The wire is located between the membrane and the E-tek backing plus electrode.

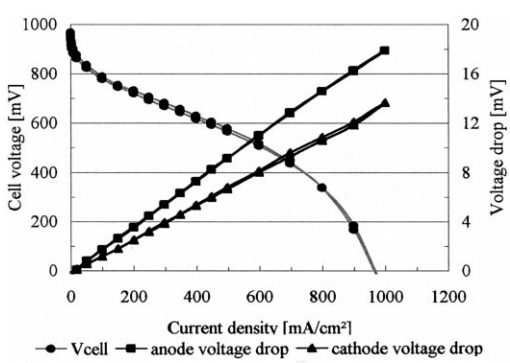

Fig. 4. Cell voltage and voltage drop over backing and contact as a function of the current density.

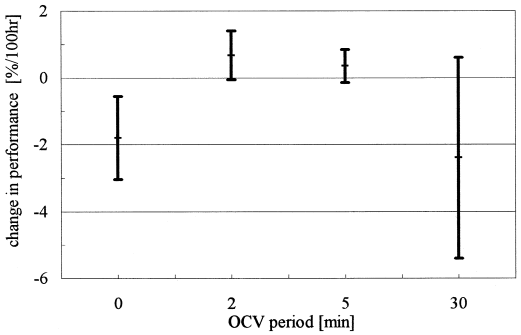

Fig. 5. Influence of length of OCV period on the cell degradation; average values depicted, error bars indicate minimum and maximum values.

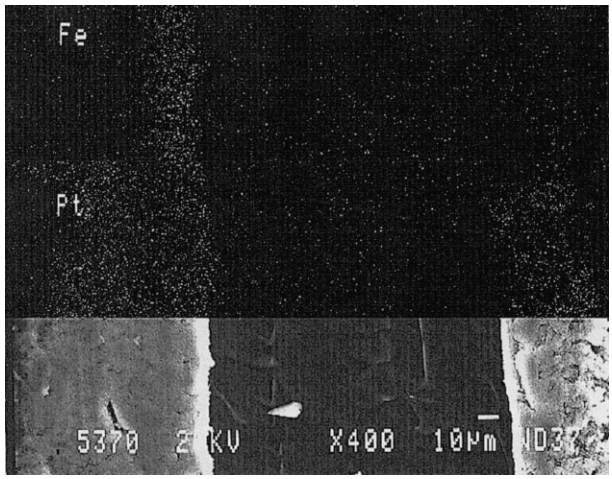

Fig. 6. SEM/EDX analysis showing a cross section of the membrane plus catalyst layers. Cathode on the left side.

Long term stability tests were carried out using the same conditions and set-up, but now with the complete flow plate constructed from the sample material. The stainless steel under consideration was only tested at either the anode or the cathode side, the other bipolar plate consisting of graphite. The materials were tested both with and without direct contact with the membrane. The temperature was reduced to 65°C to simulate the intended stack temperature.

2.3. Post-test analysis of contaminants

After the cell tests, the samples were visually and microscopically inspected for any defects. An indication of the chemical stability of a material is the amount of stainless steel constituents deposited in the MEA during the test. Therefore, the MEAs were analysed for contaminants using AAS/ICP. The resulting contaminant levels are given in mg metal per kg sample per 100 h of fuel cell operation. The target value of less than $8 \cdot 10^{-7}$ mol/cm^2 during 5000 h corresponds to 5 mg/kg per 100 h.

The chemical analyses were performed using only a part of the active cell area, i.e., the membrane, catalyst layer and backing. In order to exclude the possibility that the analytical samples were contaminated with stainless steel flakes within the backing, broken from the flow plate during sample preparation, the analyses were repeated with samples without the backing. The ratios of the contaminant levels from both analyses were 1.0 ± 0.3 for Fe, 1.3 ± 0.7 for Cr, and 1.0 ± 0.5 for Ni. These ratios are close to unity, indicating that most of the contaminants are located in the membrane and catalyst layer.

2.4. Determination of contact resistance

To determine the contact resistance between the flow plate and the backing, a thin gold wire was placed between the E-tek backing plus electrode and the membrane during assembly of the MEA, as is schematically shown in Fig. 2. In Fig. 3 a cross section of a MEA is shown, indicating the location of the gold wire.

During cell operation the voltage drop between this gold wire and the flow plate was measured. The resistance was then easily calculated from the voltage drop. Actually, the resistance also includes a contribution from the backing. It does not, however, include any polarisation effects from the electrode, as is verified by an *I–V* measurement, which is depicted in Fig. 4. While the cell voltage shows

Table 3
An overview of the test and post-test results of the different stainless steels in direct contact with the membrane. High compaction pressure of 30 bar(g) was used

Material	R_{anode} after 350 h (mΩ cm^2)	$R_{cathode}$ after 350 h (mΩ cm^2)	Metal concentrations in MEA, per 100 h of operation		
			Fe (mg/kg)	Cr (mg/kg)	Ni (mg/kg)
Graphite	10	10	< 1	< 1	< 1
1.3974	10	10	200	100	50
1.4404	10	25	500	50	50
1.4439[a]	6	6	1000	200	200
1.4529	10	10	500	100	100
1.4541[a]	20	30	1000	200	100
Alloy A	10	10	500	200	100
Alloy B	10	10	200	50	100

[a] Clear indication of pitting corrosion observed.

Table 4
An overview of the test and post-test results of the selected stainless steels using a low compaction pressure of 4 bar(g)

Material	R_{anode} after 350 h ($m\Omega\ cm^2$)	$R_{cathode}$ after 350 h ($m\Omega\ cm^2$)	Metal concentrations in MEA, per 100 h of operation		
			Fe (mg/kg)	Cr (mg/kg)	Ni (mg/kg)
Graphite	12	13	40	5	15
1.3974	35	50	200	100	75
1.4404	25	50	200	60	35
Alloy A	30	50	30	10	25
Alloy B	25	55	50	10	35

activation control at the lower current densities and diffusion control at the higher current densities, the voltage drop over the backing and the contact is a straight line, i.e., showing an ohmic behaviour.

2.5. Alternating load

In the course of these experiments, it was observed that cells showed degradation, which seemed to be influenced by the length of the OCV period. A number of experiments were carried out using graphite flow plates to investigate this phenomenon by determining the degradation for OCV periods of 0, 2, 5 and 30 min. The resulting degradations are shown in Fig. 5. No OCV period results in a degradation of about 2%; for a 30-min OCV period, the degradation amounts to 2.5%. An OCV period of 2 or 5 min results in a slightly improved cell performance. These observations can be explained as follows. Under load, the anode side of the membrane slowly dries due to the low back diffusion of water in Nafion 117. During OCV the water profile will initially change to uniform water distribution across the membrane, as there is no water drag. Therefore, for short OCV periods, the membrane will be totally hydrated. In the event of long OCV periods, the complete membrane will slowly become less hydrated due to evaporation along the edges of the cell and due to water uptake by the gases flowing across the electrodes.

3. Results

3.1. High compaction pressure, direct contact between bipolar plate and membrane

In all experiments, the decay in current density was intolerably high, approximately 30–50% in the first 300 h of operation. Only the fuel cells containing graphite bipolar plates could be operated at a fairly constant current density. The results are summarised in Table 3. For comparison, the results of tests using graphite flow plates are also included.

The first set of experiments did not favour a distinct selection of a stainless steel as bipolar plate material to be used in this fuel cell. The clear observation of pitting corrosion in the case of stainless steels 1.4439 and 1.4541 was satisfactory reason for rejection of both specimens.

The contaminant levels analysed in the spent MEAs were much higher than the target value of 5 mg/kg per 100 h. This high contamination level is thought to be one of the main causes of the large decay in cell performance observed in all tests, except for those using graphite bipolar plates.

The contact resistance, measured during cell operation, was, for most stainless steel plates, as low as in the case of graphite bipolar plates. Only in the case of 1.4541 and 1.4404, was the contact resistance after 350 h of operation 2–2.5 times higher than that of the fuel cell samples using graphite.

In order to identify the origin of the contaminants, the alloys A and B were tested at either the cathode side or the anode side using a graphite flow plate at the opposite site. The chemical analyses showed the anode side to be the major source of the contaminants.

An SEM/EDX analysis of a cross section of the MEA from a test with an alloy at the anode side identified iron to be located predominantly in the catalyst layer of the cathode (see Fig. 6).

3.2. Low compaction pressure, no direct contact between bipolar plate and membrane

For further analysis of the behaviour under low compaction pressure, the alloys A and B and stainless steel 1.3974 were selected as they showed the most promising

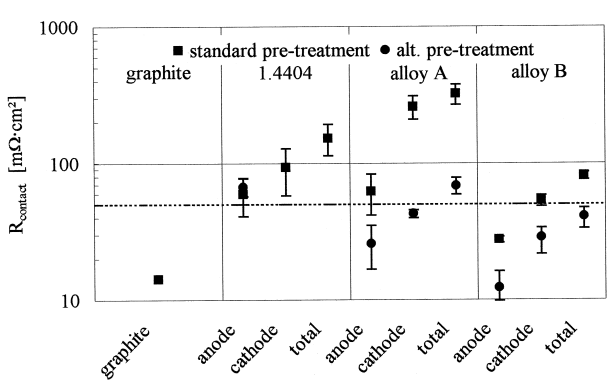

Fig. 7. The contact resistances determined after 300 h of fuel cell operation for the various materials and pre-treatments; average values depicted, error bars indicate minimum and maximum values.

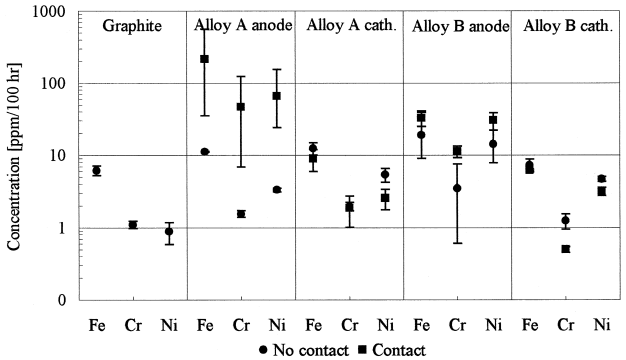

Fig. 8. Contaminant concentrations in MEA for alloys A and B, and graphite with and without direct contact between alloy and membrane; average values depicted; error bars indicate minimum and maximum values.

results under a high compaction pressure. Also, 1.4404 (SS 316L) and graphite were included in the test runs for comparison with the literature. During start-up, the compaction pressure was set to 8 bar(g); after the start-up sequence, the pressure was reduced to 4 bar(g). The results of these tests are summarised in Table 4.

The contact resistances are all comparable, but higher than for the test under a high compaction pressure. Both 1.4404 (316L) and 1.3974 show relative high contaminant levels compared to the alloys A and B. This reduces the applicability of 1.3974, and again confirms 1.4404 (316L) to be least suitable for use as bipolar plate material. For alloy A and B, the contaminant levels are largely reduced by avoiding direct contact between the acidic membrane and the stainless steel bipolar plate, and are almost comparable to the background contaminant levels, originating from the test set-up.

For all stainless steel samples, the sum of the contact resistance at the cathode side and the anode side exceeds the target value of 50 $m\Omega\ cm^2$, which is about the total contact resistance encountered when using graphite flow plates plus 25 $m\Omega\ cm^2$.

3.3. Influence of stainless steel pre-treatment

After machining and standard pre-treatment, the surface of the samples is rough and partly covered with a thin oxide layer. The nature of the surface influences the contact resistance. Therefore, the effect of an alternative pre-treatment on the contact resistance was examined for both alloys A and B and for 1.4404 (316L). For these experiments, the complete flow plate was made of the sample material. Furthermore, the OCV period was reduced from 30 min/h to 5 min/h in order to exclude any effect of membrane deterioration during the test. The tests were reformed with and without the stainless steel being in direct contact with the membrane. The contact resistances determined are depicted in Fig. 7. Included in the figure are the target values, and the results for a graphite flow plate. Also, the sum of the contact resistance at the cathode and the anode side is shown. It can be seen that the pre-treatment is of influence on the contact resistance. For the alloys A and B, the alternative pre-treatment reduces the contact resistance. Only alloy B has a total contact resistance lower than the target value; for alloy A the total resistance is slightly higher. For 1.4404 (316L) the total resistance exceeds the target value. Furthermore, the alternative pre-treatment does not seem to have a positive effect as it has for alloy A and B.

After these tests, the MEAs were analysed for contaminant levels using AAS/ICP. The results of the analyses are depicted in Fig. 8. It can be clearly seen that, in the case where the stainless steel flow plate was located at the anode side, the amount of contaminants was higher than when the stainless steel flow plate was tested on the cathode side. This is in accordance with the results obtained from the single-sided tests with a high compaction pressure. Furthermore, direct contact between the anode stainless steel flow plate and the membrane enhances the contaminant level, whereas direct contact at the cathode side does not have a significant influence. For the cathode

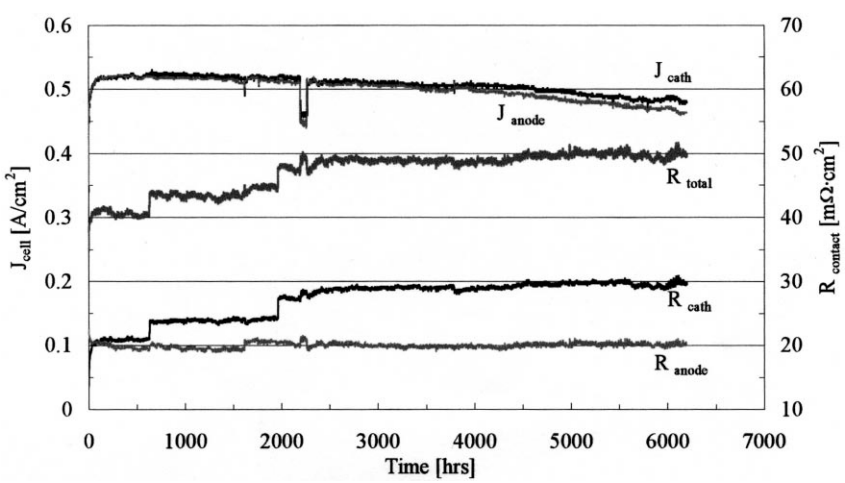

Fig. 9. Results of the endurance tests with alloy B flow plates.

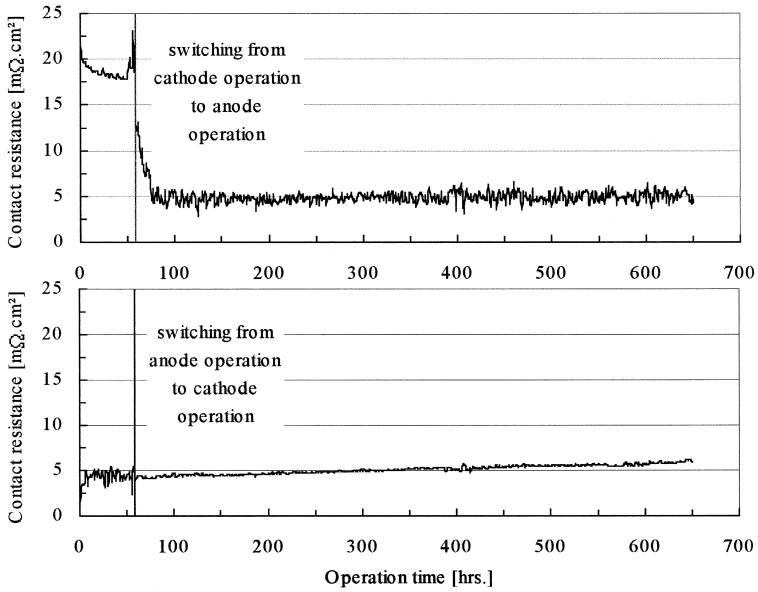

Fig. 10. The effect of interchanging the gas flows on the contact resistance; top: cathode to anode, bottom: anode to cathode.

stainless steel flow plates, the contaminant levels are comparable to the baseline values determined using graphite flow plates.

The results indicate alloy B to be most suited for application in an SPFC, as it shows the lowest contact resistance and it yields a contaminant level comparable to alloy A.

3.4. Long term stability tests

In order to verify the suitability of alloy B, two single-sided longevity tests were undertaken with an alloy B flow plate at either the cathode side or the anode side and a graphite flow plate at the opposite side, without direct contact to the membrane. The time history of both tests is shown in Fig. 9. Both cells show a stable behaviour up to about 2200 h of operation, after which both cells show an increasing degradation. The degradation of the cell with the alloy B flow plate at the anode side shows the fastest degradation.

The cell resistances show some stepwise increments which are caused by external power interruptions causing a temporary decrease in compaction pressure. Apart from these increments, the resistance at the anode side remains fairly constant, whereas at the cathode side only a minor increase is observed. Nevertheless, after 6000 h of operation, the total contact resistance is still very close to, or lower than, the allowable upper limit of 50 $m\Omega\ cm^2$.

3.5. Influence of cell reversal

During long-term stability tests, irreversible increments of contact resistance occurred. In the event the contact resistance at the cathode becomes unacceptably high, an interchange of the gas flows, i.e., making the cathode the anode and vice versa, can improve the contact resistance, as shown in Fig. 10. The decrease in contact resistance when changing the flow plate from acting as a cathode flow plate to an anode flow plate, is caused by the breakdown of the passive layer in the hydrogen-containing environment and the anode potential. The backing then contacts a bare stainless steel surface. For the opposite side, a slight increase in contact resistance is noted, caused by the formation of an oxide layer.

4. Discussion

The results of the present study indicate that the use of a stainless steel flow plate at the anode side of an SPFC results in a higher contamination of the MEA than when a stainless steel flow plate is used at the cathode side. At the cathode side, the oxide layer formed on the surface of the stainless steel protects the underlying stainless steel constituents from dissolving into the water present and, subsequently, into the membrane. At the anode side, however, no protective oxide layer will be formed due to the hydrogen-containing atmosphere and the potential appearing at that interface. The alternating load used in this study is even more detrimental to the stainless steel at the anode side, as the stainless steel will become more active during the OCV periods. When the stainless steel is in direct contact with the membrane at the anode side, the amount of contaminants in the MEA is enhanced. This agrees with the observation of Zawodzinski et al. [5], determined in out-of-cell experiments, in which an effect of the pH on

the dissolution of stainless steel constituents was observed; the membrane could be regarded as a strong acid. However, in contrast to the results of Zawodzinski et al. [2,5], appreciable amounts of stainless steel constituents were found in the MEAs after testing, including molybdenum of the order of ppm's. This is presumably the effect of the alternating load conditions used in this study.

The test results of Zawodzinski et al. [2] show lower contact resistances for SS 316 compared to our results. The main difference is the high compaction pressure used by them. The contact resistance decreases for increasing compaction pressure as can be seen in Fig. 11, and by comparing the results in Tables 3 and 4. A similar observation was made by Hornung and Kappelt [3]. Fig. 11 shows that the contact resistance increases upon lowering the compaction pressure; a subsequent increase of the compaction pressure does not result in a comparable decrease of the contact resistance. This effect was also noted during the endurance tests (Fig. 9), in which power failures and, consequently, a lowering of the compaction pressure resulted in stepwise irreversible increments of the contact resistances. A lowering of the compaction pressure results in a relaxation of compression at the backing interface and a decrease in the effective contact area, which is responsible for the increase in resistance; a subsequent increase of the pressure will increase the effective contact area, again to a similar value. However, it is likely that contact would be re-established at different points than before. A higher contact resistance, thus, indicates that the corrosion layer at these new contact points has different properties, for example, a greater thickness than at the previous contact points. Therefore, at the contact points between backing and stainless steel, a different corrosion layer would form during cell operation, than at locations where no contact was present. Moreover, the initial state of the surface represents a permanent influence on the contact resistance, as shown for the alloys A and B and the endurance tests, and also observed by Reid et al. [6]. The pre-treatment to modify the surface structure is alloy-dependent; in this study, a different pre-treatment did not affect the contact resistance for stainless steel 316L, whereas Reid et al. [6] did observe an effect for various pre-treatments.

Both Tran et al. [1] and Hentall et al. [4] concluded from their studies that bare 316 is not the optimum choice for application as flow plate material. This seems to be in line with our results regarding 316L. They concluded that gold-plated 316 is a better option. However, using this material, it will be difficult to attain a low cost bipolar plate, as the gold layer should be defect-free in order to prevent severe localised corrosion.

Both endurance tests show a decrease in performance. The cell with the alloy B flow plate at the anode side shows a larger degradation. This can be explained by the fact that the anode-side stainless steel flow plate causes a higher contamination level of the MEA, and, thus, an increase of the resistivity of the membrane, by tying up functional sites. This effect was shown to exist by Wakizoe et al. [12]. Another possibility is that an increase of the cathode polarisation resistance occurs by poisoning the Pt-catalyst, as iron can be found preferentially in the cathode catalyst layer (see Fig. 6). The sum of the contaminant levels of Fe, Cr, and Ni for alloy B amounts to more than 50 mg/kg per 100 h, as can be deduced from Fig. 8. This exceeds the target value of 5 mg/kg per 100 h by a factor 10. This target value was calculated on the assumption that all of the contaminants would tie up functional sites and, thus, result in a decrease of the membrane conductivity of at least 5% after 5000 h. The actual total contaminant level for alloy B would then result in at least a 50% decrease of the membrane conductivity, corresponding to a decrease in current density of about 100 mA/cm^2 after 5000 h. Clearly, this is not the case; only a decrease of 35 mA/cm^2 is observed. Apparently, not all of the contaminants in the MEA tie up functional sites in the membrane, which is in agreement with the preferential deposition of contaminants in the electrode layer, as shown in Fig. 6.

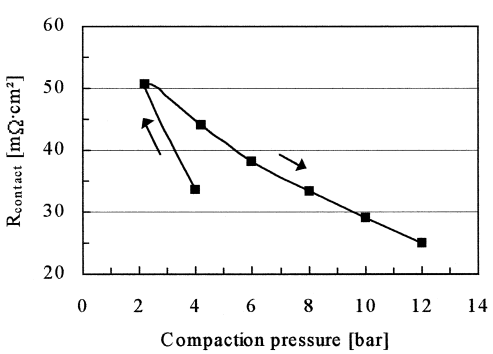

Fig. 11. Influence of the compaction pressure on the contact resistance; measurement started at 4 bar(g).

5. Conclusions

The compaction pressure is of considerable influence on the contact resistance between the electrode backing and the bipolar plate. Furthermore, the nature of the surface is also of influence; this is a permanent effect. Stainless steel constituents slowly dissolve into the MEA. The anode-side stainless steel flow plate is the main source of contaminants and they are incorporated into the membrane plus catalyst layer, preferentially in the cathode catalyst layer. Direct contact between the stainless steel and the membrane greatly enhances the contaminant level.

A variable load can be of influence on the degradation of a cell.

Using an appropriate pre-treatment and a coating, or gasket, preventing direct contact between stainless steel and the membrane, alloy B satisfies the requirements for use as a low cost material for the flow plate of an SPFC.

Acknowledgements

The work presented in this paper is funded by the EC within the JOULE III programme under contract JOU3-CT95-0027, and the Dutch Ministry of Economic Affairs.

References

[1] D.T. Tran, O.A. Velev, I.J. Kakwan, S. Gamburzev, F. Simoneaux, T.R. Lalk, S. Srinivasan, Electrochem. Soc. Abstracts, 190th Fall Meeting San Antonio 1996, Abstract 101.
[2] C. Zawodzinski, M.S. Wilson, S. Gottesfeld, Fuel Cell Seminar, Orlando, 1996, 659.
[3] R. Hornung, G. Kappelt, J. Power Sources 72 (1998) 20.
[4] P.L. Hentall, J.L. Lakeman, G.O. Mepsted, P.L. Adcock, J.M. Moore, J. Power Sources 80 (1999) 235.
[5] C. Zawodzinski, M.S. Wilson, S. Gottesfeld, Fuel Cell Seminar, Palm Springs, 1998, abstract 1191.
[6] C.E. Reid, W.R. Merida, G. Mclean, Fuel Cell Seminar, Palm Springs, 1998, abstract 1174.
[7] M. Hecht, R.O. Loufty, 33rd IECEC, Colorado Springs, 1998, Abstract 124.
[8] T.M. Besmann, J.W. Klett, T.D. Burchel, Mater. Res. Symp. Proc. Vol. 496 (1998) 243.
[9] K. Ledjeff-Hey, F. Mahlendorf, O. Niemzig, A. Trautmann, Fuel Cell Seminar, Palm Springs, 1998, abstract 1165.
[10] D.N. Busick, M.S. Wilson, Fuel Cell Seminar, Palm Springs, 1998, abstract 1186.
[11] R.K.A.M. Mallant, F.G.H. Koene, C.W.G. Verhoeve, A. Ruiter, Fuel Cell Seminar, San Diego, 1994, 503.
[12] M. Wakizoe, H. Murata, H. Takei, Asahi Chemical Aciplex-S Membrane for PEMFC, Fuel Cell Seminar, Palm Springs, 1998, abstract 1140.